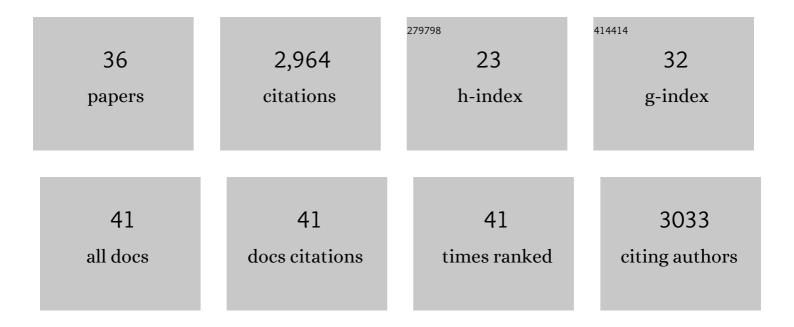
## Elsa D. Garcin

List of Publications by Year in descending order

Source: https://exaly.com/author-pdf/7420918/publications.pdf Version: 2024-02-01



FISA D CARCIN

#	Article	IF	CITATIONS
1	A fusion of the Bacteroides fragilis ferrous iron import proteins reveals a role for FeoA in stabilizing GTP-bound FeoB. Journal of Biological Chemistry, 2022, 298, 101808.	3.4	6
2	A new paradigm for gaseous ligand selectivity of hemoproteins highlighted by soluble guanylate cyclase. Journal of Inorganic Biochemistry, 2021, 214, 111267.	3.5	12
3	Quantitative high-throughput screening assays for the discovery and development of SIRPα-CD47 interaction inhibitors. PLoS ONE, 2019, 14, e0218897.	2.5	28
4	Synergistic mutations in soluble guanylyl cyclase (sGC) reveal a key role for interfacial regions in the sGC activation mechanism. Journal of Biological Chemistry, 2019, 294, 18451-18464.	3.4	8
5	GAPDH as a model non-canonical AU-rich RNA binding protein. Seminars in Cell and Developmental Biology, 2019, 86, 162-173.	5.0	40
6	Structure/function of the soluble guanylyl cyclase catalytic domain. Nitric Oxide - Biology and Chemistry, 2018, 77, 53-64.	2.7	24
7	Targeting Conformational Activation of CDK2 Kinase. Biotechnology Journal, 2017, 12, 1600531.	3.5	13
8	D-Glyceraldehyde-3-Phosphate Dehydrogenase Structure and Function. Sub-Cellular Biochemistry, 2017, 83, 413-453.	2.4	44
9	The sweet side of <scp>RNA</scp> regulation: glyceraldehydeâ€3â€phosphate dehydrogenase as a noncanonical <scp>RNA</scp> â€binding protein. Wiley Interdisciplinary Reviews RNA, 2016, 7, 53-70.	6.4	39
10	Small-angle X-ray scattering method to characterize molecular interactions: Proof of concept. Scientific Reports, 2015, 5, 12085.	3.3	33
11	A Dimer Interface Mutation in Glyceraldehyde-3-Phosphate Dehydrogenase Regulates Its Binding to AU-rich RNA. Journal of Biological Chemistry, 2015, 290, 1770-1785.	3.4	47
12	Heat Shock Protein 90 Associates with the Per-Arnt-Sim Domain of Heme-free Soluble Guanylate Cyclase. Journal of Biological Chemistry, 2015, 290, 21615-21628.	3.4	22
13	Regulation of soluble guanylate cyclase by matricellular thrombospondins: implications for blood flow. Frontiers in Physiology, 2014, 5, 134.	2.8	29
14	YC-1 Binding to the β Subunit of Soluble Guanylyl Cyclase Overcomes Allosteric Inhibition by the α Subunit. Biochemistry, 2014, 53, 101-114.	2.5	32
15	Interfacial Residues Promote an Optimal Alignment of the Catalytic Center in Human Soluble Guanylate Cyclase: Heterodimerization Is Required but Not Sufficient for Activity. Biochemistry, 2014, 53, 2153-2165.	2.5	39
16	Determining the Effect of Dithiolethione Compounds on the Activity of Human Glyceraldehyde-3-Phosphate Dehydrogenase. Biophysical Journal, 2013, 104, 232a.	0.5	0
17	Structural basis for the regulation of endothelinâ€1 mRNA stability by glyceraldehydeâ€3â€phosphate dehydrogenase. FASEB Journal, 2012, 26, 951.5.	0.5	0
18	Structural studies of the regulatory domain of bovine soluble guanylate cyclase. FASEB Journal, 2012, 26, 573.6.	0.5	0

Elsa D. Garcin

#	Article	IF	CITATIONS
19	Biochemical and structural characterization of the activation of soluble Guanylate Cyclase. FASEB Journal, 2011, 25, 959.4.	0.5	0
20	The expression, purification, and crystallization of the HNOX regulatory domain of bovine soluble guanylate cyclase. FASEB Journal, 2011, 25, 959.5.	0.5	0
21	Lys842 in Neuronal Nitric-oxide Synthase Enables the Autoinhibitory Insert to Antagonize Calmodulin Binding, Increase FMN Shielding, and Suppress Interflavin Electron Transfer. Journal of Biological Chemistry, 2010, 285, 3064-3075.	3.4	14
22	DNA apurinic-apyrimidinic site binding and excision by endonuclease IV. Nature Structural and Molecular Biology, 2008, 15, 515-522.	8.2	93
23	Anchored plasticity opens doors for selective inhibitor design in nitric oxide synthase. Nature Chemical Biology, 2008, 4, 700-707.	8.0	205
24	Biphasic Coupling of Neuronal Nitric Oxide Synthase Phosphorylation to the NMDA Receptor Regulates AMPA Receptor Trafficking and Neuronal Cell Death. Journal of Neuroscience, 2007, 27, 3445-3455.	3.6	143
25	Surface Charge Interactions of the FMN Module Govern Catalysis by Nitric-oxide Synthase. Journal of Biological Chemistry, 2006, 281, 36819-36827.	3.4	53
26	Structural differences between the ready and unready oxidized states of [NiFe] hydrogenases. Journal of Biological Inorganic Chemistry, 2005, 10, 239-249.	2.6	291
27	C-terminal Tail Residue Arg1400 Enables NADPH to Regulate Electron Transfer in Neuronal Nitric-oxide Synthase. Journal of Biological Chemistry, 2005, 280, 39208-39219.	3.4	35
28	The Three Nitric-oxide Synthases Differ in Their Kinetics of Tetrahydrobiopterin Radical Formation, Heme-Dioxy Reduction, and Arginine Hydroxylation. Journal of Biological Chemistry, 2005, 280, 8929-8935.	3.4	49
29	Structural Basis for Isozyme-specific Regulation of Electron Transfer in Nitric-oxide Synthase. Journal of Biological Chemistry, 2004, 279, 37918-37927.	3.4	244
30	Conformational Changes in Nitric Oxide Synthases Induced by Chlorzoxazone and Nitroindazoles: Crystallographic and Computational Analyses of Inhibitor Potency. Biochemistry, 2002, 41, 13915-13925.	2.5	63
31	Halophilic Adaptation:Â Novel Solvent Protein Interactions Observed in the 2.9 and 2.6 Ã Resolution Structures of the Wild Type and a Mutant of Malate Dehydrogenase fromHaloarcula marismortui‡. Biochemistry, 2000, 39, 992-1000.	2.5	104
32	The crystal structure of a reduced [NiFeSe] hydrogenase provides an image of the activated catalytic center. Structure, 1999, 7, 557-566.	3.3	448
33	Structural bases for the catalytic mechanism of NiFe hydrogenase. Pure and Applied Chemistry, 1998, 70, 25-31.	1.9	23
34	Structural bases for the catalytic mechanism of [NiFe] hydrogenases. Biochemical Society Transactions, 1998, 26, 396-401.	3.4	18
35	Hydrogenase: A hydrogen-metabolizing enzyme. What do the crystal structures tell us about its mode of action?. Biochimie, 1997, 79, 661-666.	2.6	65
36	Structure of the [NiFe] Hydrogenase Active Site:  Evidence for Biologically Uncommon Fe Ligands. Journal of the American Chemical Society, 1996, 118, 12989-12996.	13.7	657